

## **Pointing and Alignment of the CDS Grazing Incidence Spectrometer on SOHO**

N.P.M. Kuin and G. Del Zanna  
Mullard Space Science Laboratory,  
University College London,  
Holmbury St. Mary, Dorking, Surrey RH5 6NT, UK  
Tel.: +44 (0) 1483 204295(NPMK)  
Fax: +44 (0) 1483-278312

Email: [npmk@mssl.ucl.ac.uk](mailto:npmk@mssl.ucl.ac.uk) (Paul Kuin)  
and  
[gdz@mssl.ucl.ac.uk](mailto:gdz@mssl.ucl.ac.uk) (giulio Del Zanna)

# Pointing and Alignment of the CDS Grazing Incidence Spectrometer on SOHO

This version dated: 13 February 2006

**Abstract** The pointing of the Grazing Incidence Spectrometer (GIS) on the SOHO CDS instrument has been determined by study of the limb data, and has been compared to the pointing of the Normal Incidence Spectrometer (NIS). The results show that the size of the solar image seen by both instrument is the same, but since the SOHO attitude loss incident in June 1998 the GIS observes the sun at a different position, shifted 20.2 arcsec to the south, for zero roll angle, compared to the NIS. No evidence for a distortion of the rastered image of the sun in GIS data was found.

## 1 Introduction

The Coronal Diagnostic Spectrometer (CDS) on board of the SOHO observatory [3] consists of two spectrometers, the NIS and GIS, with common telescope, aperture, scan mirror, and slit. Gratings and detectors differ between NIS and GIS. The NIS provides imagery in the EUV of selected solar regions with limited spectral coverage in the 30.8-37.9 nm and 51.3-63.3 nm ranges, while the GIS provides a high resolution spectral coverage in four bands around 15.1-22.1 nm, 25.6-34.1 nm, 39.3-49.2 nm, and 65.9-78.5 nm. The precise ranges depend on operational parameters which slowly change over time.

Many lines of important atomic transitions occurring in the solar transition region and corona, are present in these EUV spectral bands. They provide the ability to study temperatures and densities of the solar plasma.

To take full advantage of the imaging and spectral capabilities of CDS, a knowledge of the relative pointing and alignment between the GIS and NIS is desirable. That is the subject of this study. The CDS absolute pointing is accurate within 10 arcsec, while stability over a period of 15 minutes is within 1 arcsec [3]

---

Address(es) of author(s) should be given

Loss of attitude of SOHO in June 1998 caused irreversible changes to the instruments. The changes to the intensity response and wavelength calibration have been reported by [2], [4], [1]. The pointing of the CDS can be monitored using a sun sensor, while the NIS pointing can be verified independently from the daily SYNOP\_F north-south central meridian and monthly full disk synoptic monitoring programs. The GIS pointing, not being an instrument that can easily build up large, high resolution, rasters due to the time needed to do so, has been more difficult to pin down. In the current study use is made of GIS rasters which cross the limb. Since each raster consists of many spectra, the fall-off in intensity over the limb can be studied for selected spectral lines. The spectral line selections will be detailed further below.

A GIS raster is usually built up by moving the scan mirror in 2" steps for east-west scans and by using the slit mechanism in 1" steps for north-south scans. Another way of building up a raster exists by controlling the pointing of the whole CDS instrument independently of the spacecraft. This is done by controlling the length of the bolts that attach the CDS to the spacecraft. The latter method is not preferable since the pointing shows some error that may be due to hysteresis [6].

The possibility exists, that the image formed by the rasters has become distorted due to degradations in the mirror or slit mechanism movement. This would lead to a varying error in limb position around the sun. We study the distortion of the limb imaged by GIS using the available limb data.

In discussing the direction of scanning, we are assuming that the spacecraft roll angle is 0.0 degrees, the default. If not, the raster will be rotated in the sun by the roll angle. This is relevant in one particular way. Due to loss of telemetry from the main antenna, SOHO now observes half the time with 180 degree roll angle, which inverts the north and south, east and west. It also inverts any solar image shift observed, as that shift is internal to the instrument, and rotates with it. We included the roll angle in the present study.

The pointing of the CDS is derived from the attitude and pointing data of the SOHO platform and the CDS pointing relative to the platform. The pointing data is obtained by software common to NIS and GIS and is processed by software common to NIS and GIS and is stored in the FITS header of the CDS data files. Corrections that are found to be necessary are maintained in the solarsoft software, and applied when reading the data with 'cdsreadfits'.

## 2 Methodology for determining the solar limb in CDS coordinates

The solar limb position in NIS data was determined using the drop in the line intensity of the OV 629.7 A line. Typically, limb rasters in the synoptic data measure 240" by 240" and show a clear drop in intensity at the limb. Along the limb some variation in extent is seen due to the presence of different structures. The question is thus how that affects a good consistent measurement. To gain some insight in the accuracy of the limb measurements, a limb measurement was made from the browsing tool at a place where there

**Table 1** Selected spectral lines. *wavelength in Angstrom*

Quality	$\langle\lambda\rangle$	$\lambda_{min}$	$\lambda_{max}$	$\Delta\lambda$	Ion	Detector
good	465.3	464.5	466.0	1.5	NeVII	3
very good	760.4	759.8	761.8	2.0	OV + OV	4
very good	765.3	764.5	765.9	1.4	NIV	4
good	718.6	718.1	719.5	1.4	OII	4
good	685.5	684.5	687.0	2.5	NIII triplet	4
variable	304.1	303.4	305.1	1.7	HeII	2
poor	275.5	275.1	266.0	0.9	SiVII	2

appeared to be a minimum in activity above the limb and around the same position as the corresponding GIS spectral scan was made. The limb position error due to variation in activity along the normal quiet sun polar limb is judged to be about 4".

The solar limb position in GIS and NIS data was found by selecting rasters that cross the limb. For the NIS a section of the image along the N-S axis was selected, where, to reduce the effect from the activity variation on the limb, a strip 20 pixels wide along the central meridian was integrated in the E-W direction. For the GIS, the intensity of selected lines was plotted. Low excitation lines were chosen because their emission drops off closer to the limb. The line intensity on the disk varies due to activity. At and near the limb brightening occurs that is due to the projection effect and the fact the source is optically thin. A concern is that in the presence of activity at the limb the location of the drop in intensity will be affected, as well as the magnitude of the brightening. In our judgement the effect of the enhanced brightening of the limb emission in active regions might pose a problem for a consistent determination of the limb. We decided to adopt a measurement based on the point where the intensity dropped below the intensity variations seen on disk. That may result in an overestimate of the true limb position, but it is a well defined and reproducible measure which is sufficient for the goals of the present study. The same limb measurement method was used for NIS and GIS data. The use of several spectral lines in GIS data allowed for the determination of an error in the measurements, which varied according to the activity on the limb, typically between 2" and 4". It also should be noted that the lower excitation species provided limb position measurements smaller than the higher excitation species. The positions reported refer to the N iv and O v data which were chosen because both NIS and GIS have O V data.

The selected spectral lines are given in table 1. along with the wavelength ranges within which the intensities were integrated. These included some lines that were not directly useful; specifically, HeII 304 shows much variation that alert for the presence of activity, and SiVII has emission extending much further out than OV and also tends to be more sensitive for changes in coronal emission.

In the selection of the wavelength integration ranges [ $\lambda_{min}, \lambda_{max}$ ] the consideration was foremost to select emission that would allow the determination of the limb to be done accurately. Therefore, the GIS intensities

used were not recalibrated or smoothed. The NIS data were fully calibrated. The wavelength range around 760 Angstrom thus contains the contribution of two OV lines, while the wavelength range around 685 Angstrom contains three weak NIII lines. Although noisy, their intensities show a clear drop at the limb and are thus well suited for this study. The column named 'Quality' is our indication of the suitability of that line for determining the limb.

The GIS lines of OV and NIV showed consistently a well defined intensity drop that was the same at both north and south limb. They carried the most weight in our measurements, while the lines of NIII and OII were used for corroboration, mostly because they tend to be more noisy due to low count rates. The NeVII line shows more variation in the slope of the intensity fall-off which is attributed to activity, gives results consistent with the other lines, and deviations were interpreted as giving an indication of the error due to extended emission above the limb.

### 3 Measurement of the North and South Polar Limb Positions

Early on in our measurements we looked at some 2004 GIS limb data which clearly showed an offset to the south for the default roll angle (0.0 deg.). An alternative way was developed to measure the limb offsets and cross-section of the sun by plotting the spectral line intensities from the GIS limb rasters as a function of radius. For example, in the N-S limb study, one can think of this as folding the south limb data over the equator to overlap the north limb data. If there is a shift of the GIS to the south, this shift becomes then twice amplified in the overlay. In figure 1 this process has been depicted. Hence it allows for a more accurate determination of the shift between the north and south limb in GIS data, by shifting the limbs until they match, and measuring the required shift. In this way most of the GIS N-S data of table 2 were obtained. Before 2001 there were no data that included both north and south limbs within a short period, and there the limb measurements have been compared between NIS and GIS for one limb at a time. For the north-south limb measurements the NIS synoptic daily data were used; for GIS a variety of data, including the SPECT\_4 synoptic program data were used.

The difference between the NIS and GIS limb positions is shown in figure 2. There is a mean shift of the GIS from NIS to the south of  $22 \pm 2.1''$ , and a mean shift from NIS the North of GIS of  $18.8 \pm 3.8''$ . They are not equal, but the mean shift of GIS is by  $20.2''$  in the southward direction. The difference between the north and south limb measurements of NIS only showed a small bias of  $-1.1''$  in our sample. We note that this may be due to selection effects, since only NIS data were used when GIS limb measurements were available. A small net difference in solar diameter measurements of NIS and GIS of  $3.2''$  could be inferred if the errors due to varying activity between the solar poles would be negligible. We note however, that long lasting coronal holes do not affect both north and south pole the same way, and a  $3.2''$  shift in the measurements is quite within the expected errors for the limb data we inspected.

In figure 3 the measured diameter from the N-S limb positions is used to plot the observed limb radius  $R_{limb}$  for both NIS and GIS in panel a, and the

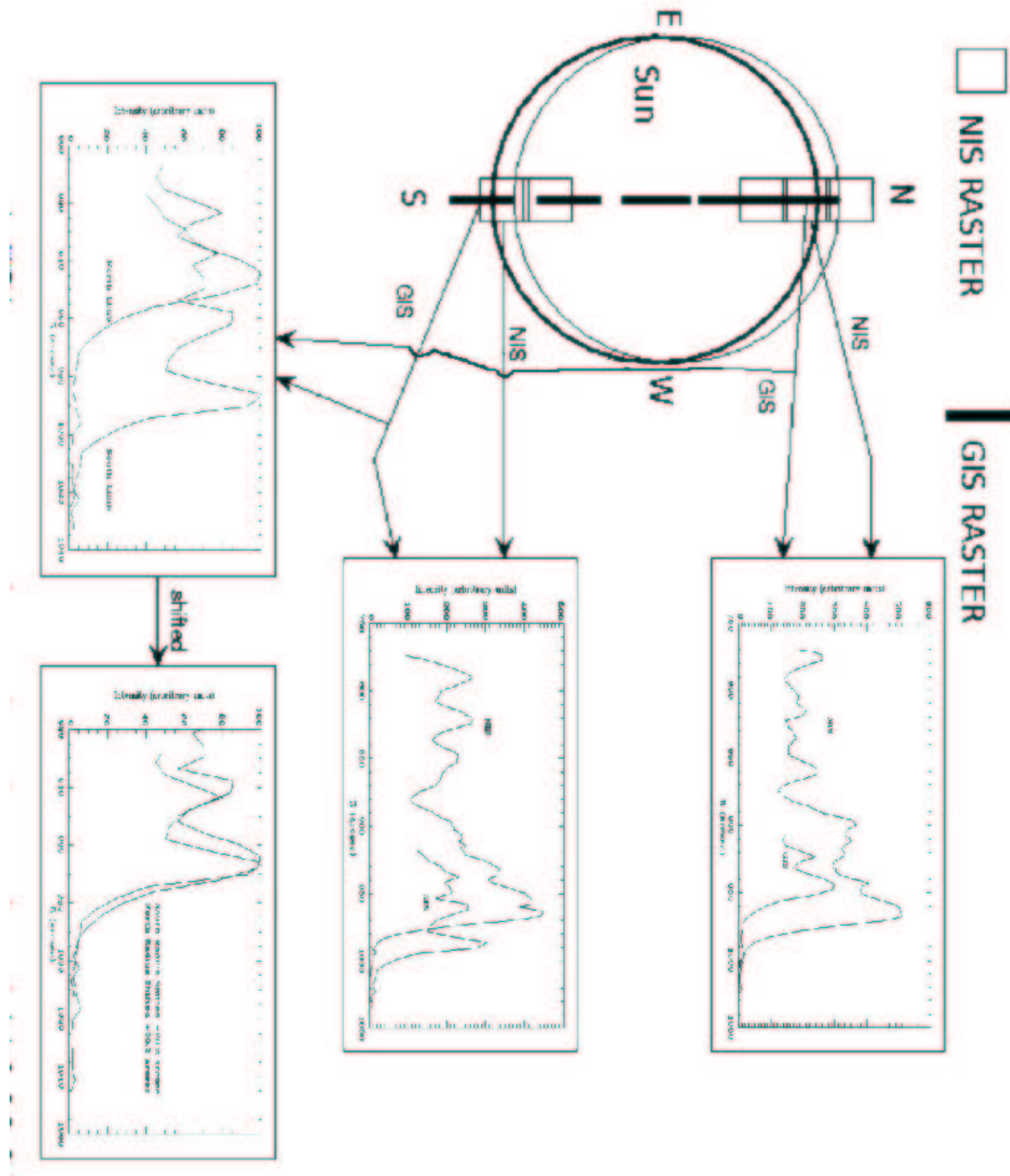


**Fig. 1** Overview of the use of GIS and NIS rasters that cross the limb for determining the limb position. Intensities (in arbitrary units) are plotted as a function of radius following Eq. 1.

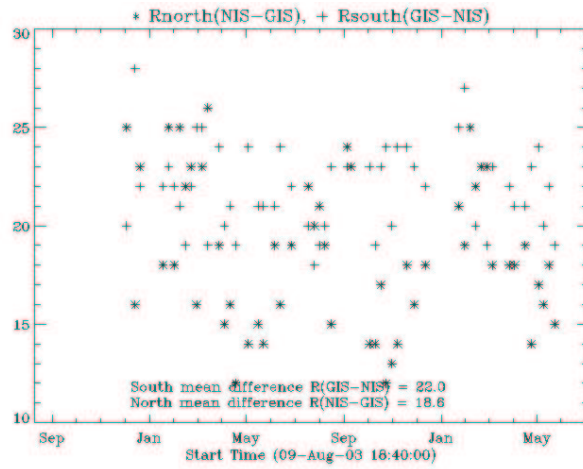


**Fig. 2** The measured limb radii difference between NIS and GIS measurements for north and south limb separately plotted.

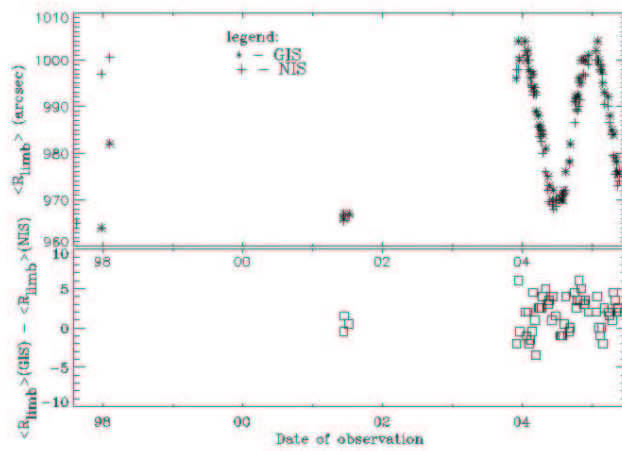


**Fig. 3** a. The measured limb radius for NIS and GIS (GIS corrected for shift); b. The difference between the measured radius of NIS and GIS.

difference between NIS and GIS in panel b. Due to the orbital motion of the earth L1 point around the sun, the radius seasonally changes as is clear from panel a, while comparison to panel b shows that the net difference between the NIS and GIS limb is uncorrelated to that variation in limb radius.

#### 4 Limb position measurements around the limb

In a similar way to the N-S measurements, the east-west limbs were measured. Only a few coeval GIS measurements of both limbs are available. The

data taken in October 1997 show no east-west shift; a recent measurement (November 2005) shows a 6 arcsec shift. All other GIS limb data since June 1998 were processed. The method followed started with a search through the header catalog to find all GIS data in the general area of the limb. A further selection based on the length of the raster was required. The limb was measured using the same procedure as before, but now on just one limb. Unfortunately, not many observations were without problem, because the observing programs tend to prefer limb activity. Some problematic data were found. Some data did not cross the limb, or showed extreme intensities due to flaring. Several also crossed filaments at the limb, thereby making it necessary to attempt to overlay the GIS and coeval NIS data in order to discriminate between limb and filament. A closer attention to the intensity values and comparison to non-problematic data resulted in a small selection of useful limb data. The measurements can be found in tables 3 and 4.

Using the measured limb position in solar X- and Y- coordinates, uncorrected, as provided by the current solarsoft readcdsfits software, we can derive the radius and angle that would correspond to these X,Y coordinates. In the absence of any shifts, the angle derived from these coordinates would be the actual angle from the north pole to the limb, and the radius should be the same around the limb (apart from the solar oblateness that we can neglect here). In actuality the GIS solar limb is not centered in the X,Y coordinates and thus we can plot the resulting difference from the expected solar radius as a function of angle,

$$R_{obs} = \sqrt{(X^2 + Y^2)}, \phi = \arctan(X/Y) \quad (1)$$

In figure 4 the limb data are plotted using polar coordinates. Due to the SOHO/Earth orbital motion the measured radii had to be normalised to the Photospheric solar radius  $R_{sun}$  as seen from SOHO which was calculated from date and orbital elements by a solarsoft routine called Pb0r. The data show a cosine dependence and an upward shift. As can be seen from figure 5, the ratio of the limb measured here to the solar photospheric radius  $R_{sun}$  is larger than 1 percent, but there is a large spread so that the mean multiplication factor is  $1.017 \pm 0.005$ .

The difference between the observed radius at the top of the lower transition region and the photospheric radius shown in Figure 4 would be zero for no image shift and identical radius. A little math shows that the following equation applies for small shifts and radial changes:

$$(R_{obs} - R_{sun})/R_{sun} = \delta R + (Y_{shift}/R_{sun}) \cdot \cos(\phi) \quad (2)$$

where  $\delta R$  is the difference in radius relative to the photospheric radius and  $\phi$  is the angle to the limb crossing measured clockwise from the north. With values for  $\delta R = 0.010$ ,  $Y_{shift} = 20.2/R_{sun}$ , and setting  $R_{sun} = 1000$  in the last factor, a reasonable approximation to these data can be found. The  $\delta R$  derived from the mean limb data in figure 5 would be too high. This may not be inconsistent. A  $\delta R$  value of 0.010 is a lower bound and the larger values may be due to more activity above the limb. There is also a selection effect. The N-S data are mostly from 2004 and 2005, while the data around the limb are more spread out over the period 1998-2005. In figure 4 there



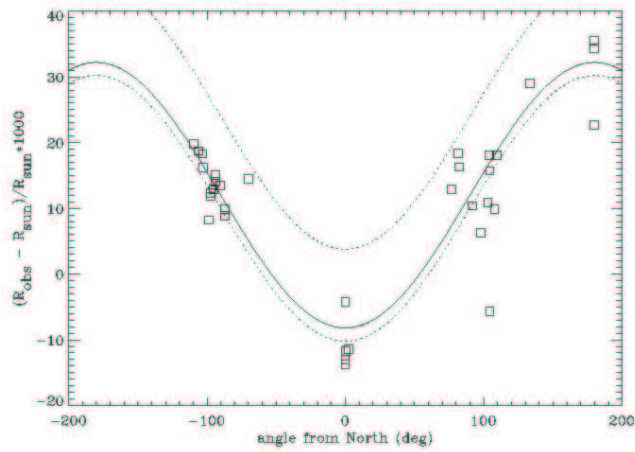


**Fig. 4** measured limb radius relative to the expected solar radius as a function of the angle from the north

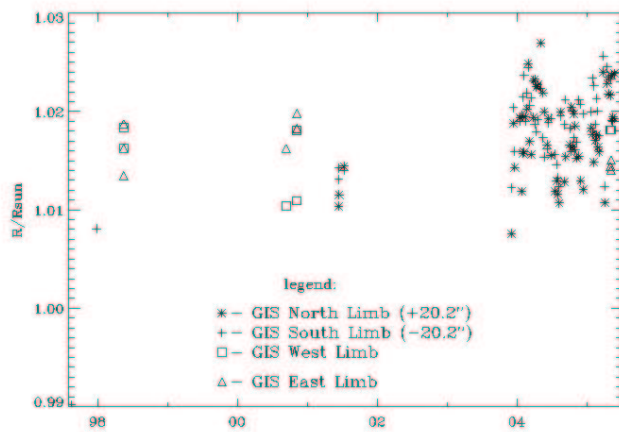


**Fig. 5** measured limb radius relative to the solar photospheric radius

is one measurement that is a clear outlier, which involves a nearby active filament that may obscure the limb, but the comparison to earlier NIS data seemed to indicate the filament was not at that position.

## 5 Discussion

The limb data do not show a GIS shift between the east and west limb, or a radius that is different around the limb. Also, comparisons to NIS polar limb data show no difference between NIS and GIS apart from a well-established image shift.

The difference in limb measurements for the different lines in GIS shows that the GIS data can be used for study of the extent of the limb emission.

The data show that the limb in the EUV lines of OV extend above the photosphere  $R_{sun}$ . The height of the lower transition region, and its extent in OV have been determined hereby to be  $0.017 \pm 0.005$  solar radii, or  $1.2 \times 10^4$  km. Since OV is formed at temperatures up to  $3 \times 10^5$  K, the top of the observed limb in OV is only slightly larger than the scale height at those temperatures. As [5] showed, cool loops that exceed the scale height become thermally unstable. The observed limb is thus consistent with theoretical expectations.

## 6 Conclusions

The pointing of the GIS instrument differs from the NIS by viewing the solar image shifted to the south, i.e., with north and south limb having a position in the solar-Y coordinate that is, on the average,  $20.2''$  less.

Based on measurements of the limb the GIS and NIS see the same size solar image, without measurable distortions.

A procedure to correct the GIS data will be provided in solarsoft.

## 7 Acknowledgements

Paul Kuin wishes to thank his colleagues at MSSL for a great atmosphere, and too many others to mention.

## References

1. del Zanna, G.: 2002, *The Radiometric Calibration of SOHO, ISSI Scientific Report SR-002. Edited by A. Pauluhn, M.C.E. Huber and R. von Steiger. ESA Publications Division, Noordwijk, The Netherlands, 2002., p.283, 283.*
2. Del Zanna, G., Bromage, B.J.I., Landi, E., and Landini, M.: 2001, *Astron. Astroph.*, **379**, 708.
3. Harrison, R.A., Sawyer, E.C., Carter, M.K., Cruise, A.M., Cutler, R.M., Fludra, A., Hayes, R.W., Kent, B.J., Lang, J., Parker, D.J., Payne, J., Pike, C.D., Peskett, S.C., Richards, A.G., Culhane, J.L., Norman, K., Breeveld, A.A., Breeveld, E.R., Janabi, K.F.A., McCalden, A.J., Parkinson, J.H., Self, D.G., Thomas, P.D., Poland, A.I., Thomas, R.J., Thompson, W.T., Kjeldseth-Moe, O., Brekke, P., Karud, J., Maltby, P., Aschenbach, B., Brauningner, H., Kuhne, M., Hollandt, J., Siegmund, O.H.W., Huber, M.C.E., Gabriel, A.H., Mason, H.E., and Bromage, B.J.I.: 1995, *Solar Phys.*, **162**, 233.
4. Lang, J., Thompson, W.T., Pike, C.D., Kent, B.J., and Foley, C.R.: 2002, *The Radiometric Calibration of SOHO, ISSI Scientific Report SR-002. Edited by A. Pauluhn, M.C.E. Huber and R. von Steiger. ESA Publications Division, Noordwijk, The Netherlands, 2002., p.105, 105.*
5. Martens, P.C.H. and Kuin, N.P.M.: 1982, *Astron. Astroph.*, **112**, 366.
6. Thompson, W.T.: 1999, *CDS Pointing Calculations, CDS Software Note No. 48. SOHO Project, 27 January 1999, p1-6.*

**Table 2** North-South Limb measurements and derived parameters

CDS ID	Roll	$R_{phot}$	$R_{meas}$	$Y_{shift}^{(n)}$	$R_S^{GIS}$	$R_N^{GIS}$	NIS ID	$R_N^{NIS}$	$-R_S^{NIS}$	date
8871	0	954.19	954.0	-11.0	965	0	8869	965		1997-08-15
10069	0	964.03	964.0	-5.0	992	0	10070	997		1997-12-26
10376	0	982.63	982.0	-5.0	0	-1008	10371	998	-1003	1998-02-08
22663	0	954.31	966.0	-21.5	987	944	22667	967	-966	2001-06-14
22672	0	954.21	967.0	-21.5	988	945	22667	968	-963	2001-06-15
22825	0	953.44	967.0	-20.0	987	947	22822	968	-965	2001-07-11
29104	0	985.72	996.0	-22.5	1018	973	29106	998	-998	2003-12-03
29205	0	984.70	1004.0	-21.0	1025	983	29206	999	-997	2003-12-14
29239	0	985.10	1000.0	-21.0	1021	979	29238	1002	-999	2003-12-20
29362	180	985.10	1004.0	20.0	1024	984	29363	1002	-1002	2004-01-18
29405	180	984.50	1000.0	24.0	1024	976	29403	1001	-1001	2004-01-25
29457	180	983.70	1002.0	23.0	1025	979	29461	997	-1003	2004-02-01
29500	180	978.64	998.0	24.0	1022	974	29501	999	-1001	2004-02-08
29555	180	977.22	996.0	20.0	1016	976	29556	998	-997	2004-02-15
29603	180	973.48	994.0	21.0	1015	973	29604	996	-993	2004-02-22
29629	180	973.00	997.0	20.0	1017	977	29630	993	-992	2004-02-29
29685	180	975.67	994.0	22.0	1016	972	29686	995	-991	2004-03-07
29753	180	971.02	989.0	23.0	1012	966	29754	992	-993	2004-03-14
29827	180	967.42	988.0	22.0	1010	966	29828	985	-986	2004-03-28
29854	0	965.74	986.0	-18.0	1004	968	29855	983	-984	2004-04-04
29908	0	965.47	985.0	-18.0	1003	967	29909	983	-982	2004-04-11
29948	0	963.34	984.0	-18.5	1002	965	29947	977	-983	2004-04-18
30008	0	957.39	981.0	-18.0	999	963	30007	977	-975	2004-05-04
30100	0	956.25	975.0	-18.0	993	957	30098	972	-972	2004-05-16
30150	0	956.10	973.0	-18.0	991	955	30151	969	-970	2004-05-23
30239	0	954.33	970.0	-20.0	990	950	30231	969	-969	2004-06-06
30325	0	953.82	972.0	-20.0	992	952	30326	968	-968	2004-06-13
30392	180	953.39	970.0	22.0	992	948	30393	967	-970	2004-06-27
30539	180	956.83	970.0	22.0	992	948	30540	970	-972	2004-07-18
30576	180	956.83	970.0	21.0	991	949	30577	969	-973	2004-07-26
30629	180	958.11	970.0	21.0	991	949	30630	970	-972	2004-08-01
30744	180	960.93	972.0	21.0	993	951	30745	970	-973	2004-08-08
30849	180	957.10	976.0	20.0	996	956	30850	971	-973	2004-08-16
31008	180	962.82	978.0	23.0	1001	955	31009	979	-978	2004-09-05
31038	180	964.36	982.0	23.0	1005	959	31039	982	-982	2004-09-10
31134	0	974.00	991.0	-21.0	1012	970	31135	984	-989	2004-10-03
31190	0	974.26	992.0	-18.0	1010	974	31191	988	-991	2004-10-10
31281	0	974.26	992.5	-22.0	1014	970	31279	987	-991	2004-10-17
31338	0	977.85	996.0	-19.0	1015	977	31340	989	-991	2004-10-24
31398	0	978.08	995.0	-19.0	1014	976	31399	989	-994	2004-10-31
31439	0	984.20	1000.0	-21.0	1021	979	31440	993	-997	2004-11-07
31541	0	982.00	1000.0	-23.0	1023	977	31535	995	-999	2004-11-19
31624	0	983.43	1000.0	-24.0	1024	976	31625	992	-1001	2004-11-28
31707	0	985.33	1001.0	-24.0	1025	977	31708	995	-1003	2004-12-12
31917	180	983.17	1002.0	21.0	1023	981	31918	1002	-998	2005-01-23
31963	180	983.80	1004.0	23.0	1027	981	31964	1000	-1000	2005-01-30
32011	180	981.63	1000.0	24.0	1024	976	32012	1001	-999	2005-02-06
32059	180	980.47	998.0	21.0	1019	977	32060	999	-999	2005-02-13
32107	180	978.93	998.0	22.0	1020	976	32108	999	-997	2005-02-20
32149	180	977.21	995.0	22.0	1017	973	32150	996	-998	2005-02-27
32193	180	976.70	993.0	21.0	1014	972	32194	990	-991	2005-03-06
32280	0	967.98	992.0	-21.0	1013	971	32281	989	-991	2005-03-27
32334	0	976.71	988.0	-21.0	1009	967	32335	985	-988	2005-04-03
32413	0	962.21	985.0	-21.0	1006	964	32414	983	-985	2005-04-16
32467	0	962.21	984.0	-21.0	1005	963	32468	977	-982	2005-04-24
32554	0	957.49	979.0	-21.0	1000	958	32555	975	-976	2005-05-03
32603	0	957.49	978.0	-18.0	996	960	32604	976	-976	2005-05-09
32640	0	956.62	975.5	-20.0	995	955	32641	973	-973	2005-05-16
32683	0	955.38	976.0	-18.0	994	958	32685	973	-975	2005-05-23

Here  $R_{phot}$  is the photospheric radius as derived from the orbit of SOHO;  $R_{meas}$  is the measured extent of the chromosphere in OV;  $R_S$  and  $R_N$  are the measured radius in OV at North and South pole, uncorrected for shift.

**Table 3** East-West Limb Measurements.

Obs.No	west limb	east limb	SC roll	west X	east X	$R_{sun\ soho}$	GIS or NIS	date
1	s4197r00	s4171r00	0	967	-963	956.7	G	1996-08-15&13
1	s4201r00	s4174r00	0	961	-973	956.7	N	1996-08-15&13
2	s9354r38	s9354r30	0	977	-980	969.5	N	1997-10-06
2	s9491r00		0	983		973.3	G	1997-10-19
2		s9517r02	0		-983	974.7	G	1997-10-19
3	s20514r00	s20515r00	0	982	-982	963.0	G	2000-09-11
4	s33951r00	s33949r00	0	982	-994	982.0	G	2005-11-25

The observation number has been introduced to make clear which observations have been combined in our analysis. West X and east X are the solar X coordinates.

**Table 4** Limb Measurements at other locations

CDS ID	roll	$R_{soho}$	Raster	N	$R_{meas}$	$\phi$ (rad)	date(s)
s11140r00	0	958.4	X	244	976.0	1.420	1998-05-17
s11140r01	0	958.4	X	244	974.0	1.437	1998-05-17
s11140r02	0	958.4	X	244	974.0	1.437	1998-05-17
s17904r00	0	976.7	X	183	995.0	-1.850	1999-11-02
s20512r00	0	963.0	Y	80	952.0	0.041	2000-09-11
s20514r00	0	963.0	X	80	973.0	1.604	2000-09-11
s20515r00	0	963.0	X	80	976.0	-1.582	2000-09-11
s21253r00	0	978.1	XY	111	994.0	-1.790	2000-11-06
s21254r00	0	978.1	XY	80	994.0	-1.795	2000-11-06
s21265r00	0	978.3	X	80	989.0	1.797	2000-11-07
s21266r00	0	978.3	X	80	996.0:	1.910	2000-11-07
s21287r00	0	978.6	X	80	996.5	-1.800	2000-11-08
s21288r00	0	978.6	X	80	998.0:	-1.910	2000-11-08
s22663r00	0	954.2	Y	244	987.0	3.140	2001-06-14
s22663r08	0	954.2	Y	244	943.0	0.001	2001-06-14
s22672r00	0	954.1	Y	244	988.0	3.140	2001-06-15
s22672r08	0	954.1	Y	244	941.0	0.000	2001-06-15
s22825r00	0	953.4	Y	244	975.0	3.140	2001-07-11
s22825r08	0	953.4	Y	244	941.0	0.000	2001-07-11
s29132r00	180	983.8	XY	60	998.0	1.920	2003-12-06
s31032r00	180	962.5	X	102	976.0	1.504	2004-09-09
s31032r01	180	962.5	X	102	977.0	1.504	2004-09-09
s31032r02	180	962.5	X	102	976.0	1.504	2004-09-09
s31032r04	180	962.5	X	102	976.0	1.504	2004-09-09
s31032r06	180	962.5	X	102	976.0	1.504	2004-09-09
s31032r08	180	962.5	X	102	976.0	1.504	2004-09-09
s31032r09	180	962.5	X	102	977.0	1.504	2004-09-09
s31662r01	0	983.3	XY	40	992.0	-1.520	2004-12-02
s31662r03	0	983.3	XY	40	993.0	-1.520	2004-12-02
s32482r00	0	963.1	X	80	971.0	-1.720	2005-04-26
s32482r11	0	963.1	X	80	971.0	-1.720	2005-04-26
s32484r00	0	963.1	X	80	975.0	-1.694	2005-04-26
s32484r11	0	963.1	X	80	974.5	-1.695	2005-04-26
s32486r00	0	963.1	X	80	975.5	-1.662	2005-04-26
s32574r11	0	960.6	X	80	978.0:	1.809	2005-05-03
s32576r00	0	960.6	X	80	978.0:	1.810	2005-05-06
s32576r11	0	960.6	X	80	978.0:	1.808	2005-05-06
s33043r00	180	954.6	XY	40	964.0	-1.260	2005-07-28
s33112r01	180	956.0	XY	200	952.0	3.140	2005-08-09
s33266r11	0	959.6	X	80	972.0	1.335	2005-08-25
s33894r00	0	981.5	X	80	1010.0	2.330	2005-11-18
s33913r00	0	981.6	X	120	976.0:	1.820	2005-11-23
s33913r03	0	981.6	X	120	997.0:	1.820	2005-11-23
s33936r00	0	981.8	X	120	988.0:	1.710	2005-11-24

Here  $R_{soho}$  is the photospheric radius as seen from the position of SOHO;  $R_{meas}$  is the measured chromospheric radius in OV,  $\phi$  is the angle of the limb position measurement clockwise from the north.